REGIONAL ANALYSIS OF LG ATTENUATION: COMPARISON OF 1-D METHODS IN NORTHERN CALIFORNIA AND APPLICATION TO THE YELLOW SEA/KOREAN PENINSULA

Sean R. Ford[1], Douglas S. Dreger[1], Kevin M. Mayeda[2], William R. Walter[3], Luca Malagnini[4], and W. Scott Phillips[5]

University of California, Berkeley[1], Weston Geophysical[2], Lawrence Livermore National Laboratory[3], Istituto Nazionale di Geofisca e Vulcanologia[4], and Los Alamos National Laboratory[5]

ABSTRACT

The measurement of regional attenuation Q^{-1} can produce method dependent results. The discrepancies among methods are due to differing parameterizations (e.g., geometrical spreading rates), employed data sets (e.g., choice of path lengths and sources), and methodologies themselves (e.g., measurement in the frequency or time domain). We apply the coda normalization (CN), two-station (TS), reverse two-station (RTS), source-pair/receiver-pair (SPRP), and the new coda-source normalization (CS) methods to measure Q of the regional phase, Lg (Q_{Lg}), and its power-law dependence on frequency of the form $Q_0 f^\eta$ with controlled parameterization in the well-studied region of northern California using a high-quality data set from the Berkeley Digital Seismic Network. We test the sensitivity of each method to changes in geometrical spreading, Lg frequency bandwidth, the distance range of data, and the Lg measurement window. For a given method, there are significant differences in the power-law parameters, Q_0 and η, due to perturbations in the parameterization when evaluated using a conservative pairwise comparison. The CN method is affected most by changes in the distance range, which is most probably due to its fixed coda measurement window. Since, the CS method is best used to calculate the total path attenuation, it is very sensitive to the geometrical spreading assumption. The TS method is most sensitive to the frequency bandwidth, which may be due to its incomplete extraction of the site term. The RTS method is insensitive to parameterization choice, whereas the SPRP method as implemented here in the time-domain for a single path has great error in the power-law model parameters and η is greatly affected by changes in the method parameterization. When presenting results for a given method it is best to calculate $Q_0 f^\eta$ for multiple parameterizations using some a priori distribution. We also investigate the difference in power-law Q calculated among the methods by considering only an approximately homogeneous subset of our data. All methods return similar power-law parameters, though the 95% confidence region is large. We adapt the CS method to calculate Q_{Lg} tomography in northern California. Preliminary results show that by correcting for the source, tomography with the CS method may produce better resolved attenuation structure.

1. REPORT DATE **SEP 2007**	2. REPORT TYPE	3. DATES COVERED **00-00-2007 to 00-00-2007**

4. TITLE AND SUBTITLE	5a. CONTRACT NUMBER
Regional Analysis of Lg Attenuation: Comparison of 1-D Methods in Northern California and Application to the Yellow Sea/Korean Peninsula	5b. GRANT NUMBER
	5c. PROGRAM ELEMENT NUMBER
6. AUTHOR(S)	5d. PROJECT NUMBER
	5e. TASK NUMBER
	5f. WORK UNIT NUMBER

7. PERFORMING ORGANIZATION NAME(S) AND ADDRESS(ES) **Lawrence Livermore National Laboratory,PO Box 808,Livermore,CA,94551-0808**	8. PERFORMING ORGANIZATION REPORT NUMBER

9. SPONSORING/MONITORING AGENCY NAME(S) AND ADDRESS(ES)	10. SPONSOR/MONITOR'S ACRONYM(S)
	11. SPONSOR/MONITOR'S REPORT NUMBER(S)

12. DISTRIBUTION/AVAILABILITY STATEMENT **Approved for public release; distribution unlimited**

13. SUPPLEMENTARY NOTES **Proceedings of the 29th Monitoring Research Review: Ground-Based Nuclear Explosion Monitoring Technologies, 25-27 Sep 2007, Denver, CO sponsored by the National Nuclear Security Administration (NNSA) and the Air Force Research Laboratory (AFRL)**

14. ABSTRACT **see report**

15. SUBJECT TERMS

16. SECURITY CLASSIFICATION OF:			17. LIMITATION OF ABSTRACT	18. NUMBER OF PAGES	19a. NAME OF RESPONSIBLE PERSON
a. REPORT **unclassified**	b. ABSTRACT **unclassified**	c. THIS PAGE **unclassified**	**Same as Report (SAR)**	**10**	

OBJECTIVES

Understanding of regional attenuation Q^{-1} can help with structure and tectonic interpretation (Aleqabi and Wysession, 2006; Benz et al., 1997; Frankel, 1990), and correcting for the effects of attenuation can lead to better discrimination of small nuclear tests (e.g. Baker et al., 2004; Mayeda et al., 2003; Taylor et al., 2002). Present threshold algorithms for event identification rely on Q models that are derived differently, and the models can vary greatly for the same region. For example, recent one-dimensional (1-D) Q studies in South Korea find frequency-dependent Q_{Lg} that at 1 Hz range from 450 to 900 (Chung and Lee 2003; Chung et al., 2005). Another example is the case of Tibet where a wide variety of Q values have been reported (e.g. Fan and Lay, 2003; Xie et al. 2004). In order to reliably use reported Q estimates for either monitoring applications, or for tectonic interpretation it is essential to know the uncertainty in the estimate. Commonly, individual studies will present aleatoric (random) uncertainty, however epistemic (bias) uncertainty is not possible to assess, when only a single method and parameterization is considered. In order to better understand the effects of different methods and parameterizations on Q models, we implement four popular methods and one new method to measure Q of the regional seismic phase, Lg (Q_{Lg}), using a high-quality data set from the Berkeley Digital Seismic Network (BDSN). The CN method is implemented in the time domain for paths leading to a common station and it returns a stable Q measurement when the region near a station is homogenous. The CS method uses previously calculated coda-derived source spectra to remove the source term in the frequency domain and is best suited to calculate an effective Q for a given path. The TS and RTS methods are implemented in the frequency domain and the calculated Q is more stable due to the extraction of the source term. The RTS method produces a power-law Q with less error than the TS method due to its additional extraction of the site terms, though it is more restrictive in its data requirements. The SPRP method is the RTS method with a relaxation of the data requirements and is implemented in the time domain here.

Through this approach we identify both aleatoric and epistemic uncertainty. With a more complete knowledge of uncertainty it will be possible to better assess the results of published attenuation studies and the presented multi-method analysis procedure employed in future efforts can lead to improved estimates of regional Q.
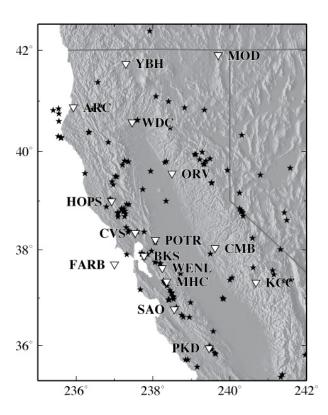

Figure 1. Events (stars), stations (inverted triangles), used in the study.

RESEARCH ACCOMPLISHED

The data set consists of 158 earthquakes recorded at 16 broadband (20 sps) three-component stations of the BDSN between 1992 and 2004 (Figure 1). The wide distribution of data parameters allows for sensitivity testing. We calculate Q_{Lg} by fitting the power-law model, $Q_0 f^n$ using five different methods. The first two methods use the seismic coda to correct for the source effect. The last three methods use a spectral ratio technique to correct for source, and possibly site effects. In the following we summarize the methods and point out significant differences. Our philosophy in presenting each of the methods is to maintain the approach and style of the popular version of each method as close as possible. Later, we will attempt to normalize each of the methods for comparison and sensitivity testing.

Coda Normalization (CN)

The CN method uses the local shear-wave coda as a proxy for the source and site effects, thus amplitude ratios remove these two effects from the S-wave spectrum (Aki, 1980; Yoshimoto et al., 1993). In his original application, Aki (1980) assumed that the local shear-wave coda was homogeneously distributed in space and time. For the current study region, Figure 1 of Mayeda et al. (2005) shows that the coda at ~1 Hz is

in fact homogeneous, at least up to ~240 km. This method assumes the *Lg* amplitude A_{Lg} at a given distance *r* and frequency *f* can be estimated by

$$A_{Lg}(f,r) = S(f)R(\theta)I(f)P(f)G(r)\exp\left(\frac{-r\pi f}{QU}\right),$$

(1)

where $S(f)$ is the source spectrum and $R(\theta)$ is the source radiation in the source-receiver direction θ. $P(f)$ is the site term, $I(f)$ is the instrument term, and $G(r)$ is the geometrical spreading term, approximated here as an inverse power-law where γ is the spreading rate and is given in Table 1. The final term is an apparent attenuation, where *U* is the *Lg* group velocity, which is fixed at 3.5 km/s for this and all other methods. The CN method also assumes that the coda spectrum $C(f)$ is approximately equal to the source spectrum at a given critical propagation time t_C. The coda excitation term is assumed to be constant at all distances for a given t_C. If the source radiation is smoothed by considering several sources at many source-receiver directions we can take the ratio of A_{Lg} to *C*, measured at t_C, which effectively removes instrument, site, and source contributions resulting in only the geometrical spreading and attenuation terms. The natural log of this spectral ratio taken at discrete frequency bands (between 0.25, 0.5, 1, 2, 4, and 8 Hz) results in the equation of a line as a function of distance and the slope is related to Q^{-1}. Q^{-1} at the center frequency of each band then reveals a power-law model for each station.

A_{Lg} is the maximum envelope amplitude in each bandpassed (8-pole acausal Butterworth filter), windowed (according to the window parameter in Table 1) and tapered raw vertical trace. *C* is the root-mean-square (rms) amplitude in each bandpassed 10 second window centered on a t_C of 150 sec. Data were excluded if either A_{Lg} or *C* had a SNR less than two, where noise is measured as the maximum amplitude in a window the same length as A_{Lg} prior to the event. This method is similar to that of Chung and Lee (2003), whereas Frankel (1990) used a weighted average of the smoothed coda to measure *C*. We calculate Q^{-1} with all records at a given station, where the slope is calculated with an iteratively weighted least-squares method. The resulting Q^{-1} are then fit in the log domain as a function of midpoint frequency with a weighted (the squared inverse of the standard error in each Q^{-1} measurement) least-squares line to calculate the power-law parameters.

Coda-Source Normalization (CS)

The CS method uses the stable, coda-derived source spectra to isolate the path attenuation component of the *Lg* spectrum (Walter et al., 2007). This method assumes A_{Lg} is represented as in equation (1) with $S(f)$ described as in Aki and Richards (2002), $G(r)$ is a critical distance formulation (Street et al., 1975). We assume a site term $P(f)$ of unity and thus any site effect is projected into the path attenuation term.

The windowed (according to the window parameter in Table 1) and tapered transverse component is transferred to velocity and its Fourier amplitude is calculated. A_{Lg} is then the mean of the Fourier amplitude for fixed discrete frequency bands (between 0.2, 0.3, 0.5, 0.7, 1, 1.5, 2, 3, 4, 6, and 8 Hz). Path attenuation can then be extracted with the log transform where the same frequency bands are used to calculate the source spectra, $S(f)$, and $P(f)$ is fixed to unity. Source spectra derived from the coda are calculated via the methodology of Mayeda et al. (2003) and from the northern California study of Mayeda et al. (2005). $Q(f)$ is only calculated for records where A_{Lg} is two times the amplitude of the pre-event signal (SNR > 2). *Q* at the center frequency of each band then reveals a power-law model for each event-station path. We fit a least-squares line in the log domain (a robust regression gave similar results) and the intercept term is then the log transform of Q_0 and the slope is η.

Table 1. Method parameterization.

Group	Spreading exponent [γ]	Measurement band (Hz)	Epicentral distance [*r*] (km)	*Lg* Velocity window (km/s)
Control	0.50	0.50–8	100 - 400	2.6–3.5
Test 1 (γ)	**0.83**			
Test 2 (Bandwidth)		**0.25–4**		
Test 3 (Distance)			**100 - 700**	
Test 4 (Window)				**3.0–3.6**

Two-Station (TS)

The TS method takes the ratio of *Lg* recorded at two different stations along the same narrow path from the same event in order to remove the common source term (e.g., Chavez and Priestley, 1986; Xie and Mitchell, 1990). We implement this method in the frequency domain and take the ratio of two terms with the form of equation (1), which can then be transformed to the log-domain and a linear regression is possible to calculate the power-law parameters. However, random error due to propagation can produce a negative argument in the exponential term of equation (1) at some frequencies (Xie, 1998), which prohibits analysis in the log-domain. Therefore, we perform a non-linear regression on the argument that minimizes the sum of squares error on the power-law function in the least-squares sense (Bates and Watts, 1988).

Reverse Two-Station (RTS)

The RTS method uses two TS setups, where a source is on either side of the station pair in a narrow azimuthal window (Chun et al., 1987). The two ratios are combined to remove the common source and site terms.

Source-Pair/Receiver-Pair (SPRP)

The SPRP method is the RTS method with a relaxation on the narrow azimuthal window requirement (Shih et al., 1994). We implement this method in the time-domain. Unlike the RTS method, data are no longer restricted by a given azimuth but by a distance formulation. A_{Lg} is the maximum zero-to-peak amplitude in each bandpassed (8-pole acausal Butterworth filter), windowed (according to the window parameter in Table 1) and tapered vertical component record that has been transferred to velocity. The equation is least-squares fit as a function of the effective interstation distance for the same discrete frequency bands as in the CN method, where *f* is the midpoint of these frequency bands. The slope of the fit is a function of Q^{-1} in the band that was measured. The resulting Q^{-1} are then fit in the log domain as a function of midpoint frequency with a weighted (the squared inverse of the standard error in each Q^{-1} measurement) least-squares line to calculate the power-law parameters.

Method Comparison

Since each method has a different data requirement it is improper to compare the methods with the full data set. For example, the CN method will sample geology at all back-azimuths relative to a station, whereas the RTS method is restricted to a narrow azimuthal window aligned roughly along a pair of stations and events.
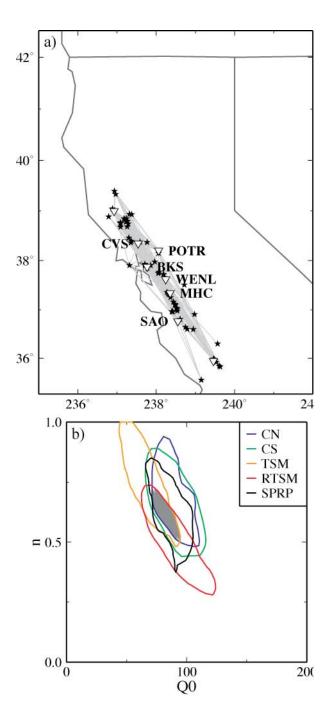

Figure 2. Method comparison. (a) Map (same region as Figure 1) of the subset used in the comparison analysis. Data are in a small region near the San Francisco Bay Area, primarily along the Franciscan block. (b) Power-law parameters and their empirical 95% confidence regions are given. The intersecting region is shaded grey.
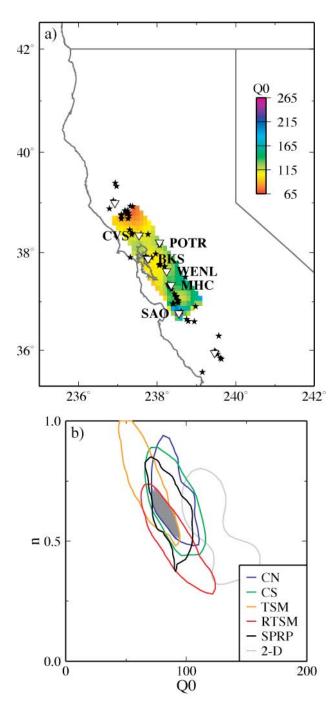
37

Figure 3. Method comparison with tomographic results of (Mayeda et al. 2005). (a) Region where 2-D direct wave attenuation coefficients are used, which covers the same area as the paths and stations in Figure 2a. (b) Comparison of tomographic results where empirical distribution (light grey) is from data at each node with 1-D results.

In an attempt to normalize the data set used for each method, we restrict the data to lie in a small region along the Franciscan block (Figure 2a). We implement all five methods to calculate $Q_0 f^\eta$ in the region (Figure 2b). The populations are then smoothed with a two-dimensional gaussian kernel (Venables and Ripley, 2002) to produce an empirical distribution so that the 95% confidence region can be estimated. The grey region in Figure 2b represents a parameter space that fits all studies. Mayeda et al. (2005) present Q tomography for Northern California in order to compare 1-D and 2-D methods to calculate both coda and direct wave (S, Lg, or surface wave) attenuation. We extend the analysis for comparison with the results from the 1-D analysis of the sub-region. Power law parameters from the Mayeda et al. (2005) study are calculated by fitting a least-squares line to the Q estimated for each frequency band at the midpoint of the band in the log domain. We extract the power-law parameters at points within the sub-region (Figure 3a) and, as above, we produce an empirical distribution (Figure 3b). The range in η and variance of Q_0 are similar between the 1-D and 2-D results, but the mean of the Q_0 distribution is shifted by about 30. This may be due to some regularization effects. This analysis shows that some of the variability in the 1-D analysis is due to 2-D structure.

Sensitivity Tests

Using the complete data set, we investigated how the choice of parameterization affects the results. In each test, only one parameter was varied, and $Q_0 f^\eta$ was calculated with each of the methods. The varied parameters are geometrical spreading rate, measurement bandwidth, epicentral distance, and the Lg window. The values of the varied parameters are listed in Table 1, where the range was chosen based on the values used in previous studies.

For the CN method, standard error regions were constructed from the covariance of the power-law model parameters estimated by bootstrapping the residuals of the weighted least-squares fit 1000 times (Aster et al., 1996). Figure 4a shows the standard error regions for each test at station PKD. All tests cluster around the control parameters except the distance test (Test 3). To assess the significance of model parameterization differences we perform an analysis of covariance (ANCOVA) for the weighted least-squares regression with Tukey's honest significant difference pairwise comparison tests (Faraway, 2004). A difference in the model parameters is only significant if the 95% confidence region of the mean difference in the model parameters between two tests does not include zero. We group all significant differences between a

given test and the control parameterization and plot the median, 25th and 75th percentile values of that group (Figure 4b). In this way, we can try and separate aleatoric uncertainty due to poorly constrained power-law model parameters and epistemic uncertainty due to the choice of parameterization for each method, and one can think of the confidence regions in panel a) of Figures 4 as the aleatoric uncertainty, and the values in panel b) as epistemic uncertainty. There is a significant difference for almost all CN method comparisons in η, and the greatest difference for both model parameters is when the epicentral distance of the data set is changed (Test 3). This is due to the fixed time t_C at which the coda is measured, where for greater distances it is more appropriate to increase t_C.

Standard error regions and pairwise comparisons are calculated for the CS method as described above, though the residuals and ANCOVA are for a direct linear regression. For most tests only a small fraction of the comparisons are significant. However, when γ is changed in Test 1, there is a significant difference in Q_0 for 39% of the path comparisons, where the median difference is almost 50. This effect highlights the difficulty in extracting an intrinsic Q from the full path attenuation when examining a single path. The CS method is best for evaluating the total path term.

Since the TS and RTS methods require nonlinear regressions, we estimate covariance matrices from the bootstrapped power-law model parameter populations. ANCOVA is performed with this estimated covariance and the pairwise comparisons are made with the results. A change in epicentral distance does not significantly affect the power-law parameters for both the TS and RTS methods, but a change in bandwidth (Test 2) produces an interquartile range of 0.05 to 0.22 for the difference in η using the TS method. The TS method is sensitive to site effects and this difference may be due to site effects that are different below 1 Hz than they are above it. For several stations in the BDSN this seems to be the case (Malagnini et al., 2007). The RTS method doesn't suffer from this same dependency and its median significant differences are low for all tests.

As previously stated, the SPRP method implemented in the time domain requires a distribution of effective interstation distances that can best be given when several interstation paths are considered. However, it should be able to constrain $Q_0 f^\eta$ for a single interstation path, and in order to allow for comparison with the implementation of the other interstation methods, TS and RTS, we carry out the method on an interstation basis. Due to such large standard error regions only around half of the pairwise comparisons give a significant difference in Q_0. However, the same comparisons reveal a large difference in η for all but the γ test (Test 1).
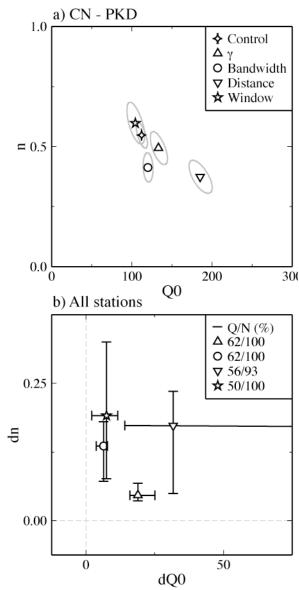

Figure 4. Parameterization effects of the coda-normalization method. a) Power-law parameters (Q_0, η) for each choice of parameterization and the standard error region. b) Results of significant difference in pairwise comparisons between the Control parameterization and its deviations (similar symbol as a) for all measurements in the method. The upper right box gives percentage of measurements that had a significant difference and the symbols are at the median difference (δQ_0, $\delta \eta$) with upper (3rd quartile) and lower (1st quartile) bounds given by the bars.
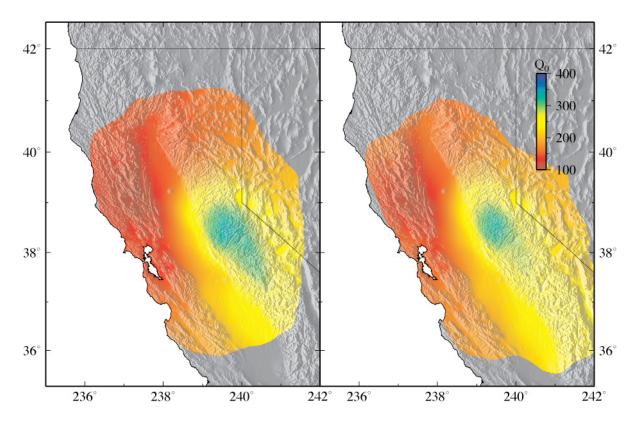
Figure 5. Attenuation tomography using amplitudes (a) where the source and site term is solved for in the inversion and (b) where the source term is removed from the amplitudes using a coda-derived moment rate.

Discussion

Each method analyzed here is employed for different types of investigation. Each method has different advantages, disadvantages and assumptions. The CN method returns a stable Q measurement when the region near a station is homogenous. The CS method is best suited to calculate an effective Q for a given path, where the site term is mapped into the path attenuation. Also, since it measures the path directly from the event to station, there is a trade-off between geometrical spreading and effective Q. If the uncertainties in the type of geometrical spreading are large, then it may be best to test several forms of spreading, or to fold the spreading term into the entire path effect if this is appropriate for the application. The CS method can be used to calculate corrected amplitudes for use in a tomographic inversion. We have created such a scheme by adapting the method of Phillips et al. (2005) and preliminary results show that this method may resolve structure more tightly (Figure 5).

The TS and RTS methods are more stable due to the extraction of the source term. The RTS method produces the least error due to its additional extraction of the site terms, though it is more restrictive in its data requirements. Xie (2002) calculates the bias due to the site term assumption in the TS method and finds that it is small. In order to test this assumption we compare the average power-law parameters for paths calculated by both the TS and RTS methods (Figure 6a). The values of the parameters are approximately the same for both methods, though there is scatter. A more direct test is to compare the power-law parameters calculated for paths to station BKS and new data from a nearly co-located BRK (Figure 6b). Malagnini et al. (2007) find a significant difference in the site term between BKS and BRK and this difference is evident in Figure 6b. Stacking ratios with common interstation paths could reduce the variance, but this is only appropriate for tectonically stable areas. Aster et al. (1996) calculates spectral ratios with the multi-taper method and is able to produce more stable spectra and a more realistic variance in the spectral measurement.

The SPRP method is the RTS method with a relaxation of the data requirements and is appropriate for very laterally homogeneous Q. The SPRP method is implemented in the frequency domain by Fan and Lay (2003), and in the time domain by Shih et al. (1994) and Chung et al. (2005), where they find clusters in small regions that are very different from the overall 1-D Q model. The SPRP method in the time domain is much better suited for a large homogeneous region, where several interstation regions can be grouped together. In the implementation here, we calculate $Q_0 f^n$ for each interstation path that fits the above criteria (<41% of the available paths), which results in pooling of data points near the true interstation distance. This can greatly effect the linear regression and produce large error in the model parameters.

CONCLUSIONS AND RECOMMENDATIONS

We apply the coda normalization (CN), two-station (TS), reverse two-station (RTS), source-pair/receiver-pair (SPRP), and the new coda-source normalization (CS) methods to measure Q_{Lg} and its power-law dependence ($Q_0 f^\eta$) in northern California in order to understand the variability due to parameterization choice and method. We investigate the reliability of the methods by comparing them with each other for an approximately homogeneous region in the Franciscan block near the San Francisco Bay Area. All methods return similar power-law parameters, especially in their 95% confidence regions. If we consider the joint distributions of each method $Q_0 = 85 \pm 40$ and $\eta = 0.65 \pm 0.35$ (both ~95% CI), where η is not as well constrained. We test the sensitivity of each method to changes in geometrical spreading, Lg frequency bandwidth, the distance range of data, and the Lg measurement window. For a given method, there are significant differences in the power-law parameters, Q_0 and η, due to perturbations in the parameterization when evaluated using a conservative pairwise comparison. The CN method is affected most by changes in the distance range, which is most probably due to its fixed coda measurement window or the fact that at larger distances the coda is not homogeneously distributed. Since, the CS method is best used to calculate the total path attenuation, it is very sensitive to the geometrical spreading assumption. The TS method is most sensitive
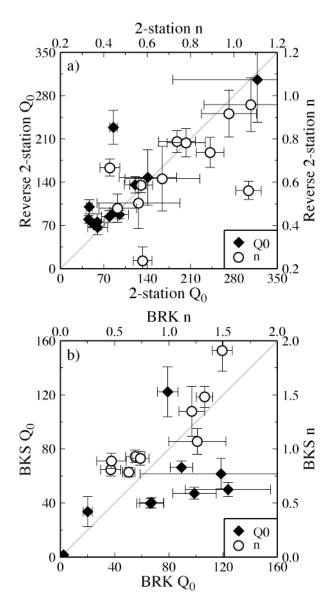

Figure 6. An investigation into site effects. (a) Power-law parameters for paths measured by both the RTS and TS methods. (b) Power-law parameters measured at nearly co-located stations BKS and BRK using the TS method.

to the frequency bandwidth, which may be due to its incomplete extraction of the site term. The RTS method is insensitive to parameterization choice, whereas the SPRP method as implemented here in the time-domain for a single path has great error in the power-law model parameters and η is greatly affected by changes in the method parameterization. When presenting results for a given method it is best to calculate $Q_0 f^n$ for multiple parameterizations using some a priori distribution. We plan to implement the methods introduced here to find 1-D and 2-D attenuation in the Yellow Sea / Korean Peninsula region.

REFERENCES

Aki, K. and P. G. Richards (2002). *Quantitative Seismology*. Sausalito, Califirnia: University Science Books.

Aki, K. (1980). Attenuation of shear-waves in the lithosphere for frequencies from 0.05 to 25 Hz, *Phys. Earth Planet. Inter.* 21: 50–60.

Aleqabi, G. I. and M. E. Wysession (2006). Q(Lg) distribution in the basin and range province of the western United States, *Bull. Seism. Soc. Amer.* 96: 348–354.

Aster, R. C., G. Slad, J. Henton, and M. Antolik (1996). Differential analysis of coda Q using similar microearthquakes in seismic gaps. Part 1: Techniques and application to seismograms recorded in the Anza seismic gap, *Bull. Seis. Soc. Amer.* 86: 868–889.

Baker, G. E., J. Stevens, and H. M. Xu (2004). Lg group velocity: A depth discriminant revisited, *Bull. Seism. Soc. Amer.* 94: 722–739.

Bates, D. M. and D. Watts (1988). *Nonlinear Regression Analysis and Its Applications*. New York: Wiley.

Benz, H. M., A. Frankel, and D. M. Boore (1997). Regional Lg attenuation for the continental United States, *Bull. Seism. Soc. Amer.* 87: 606–619.

Chavez, D. E. and K. F. Priestley (1986). Measurement of frequency dependent Lg attenuation in the Great Basin, *Geophys. Res. Lett.* 13: 551–554.

Chun, K., G. F. West, R. J. Kokoski, and C. Samson (1987). A novel technique for measuring Lg attenuation: Results from Eastern Canada between 1 to 10 Hz, *Bull. Seism. Soc. Amer.* 77: 398–419.

Chung, T. W., Y. K. Park, I. B. Kang, and K. Lee (2005). Crustal Q_{Lg}^{-1} in South Korea using the source pair/receiver pair method, *Bull. Seis. Soc. Amer.* 95: 512–520.

Chung, T. and K. Lee (2003). A study of high-frequency Q_{Lg}^{-1} in the crust of South Korea, *Bull. Seism. Soc. Amer.* 93: 1401–1406.

Fan, G. and T. Lay (2003). Strong Lg wave attenuation in the northern and eastern Tibetan Plateau measured by a two-station/two-event stacking method, *Geophys. Res. Lett.* 30.

Faraway, J. J. (2004). *Linear Models with R*. Boca Raton, Florida: Chapman & Hall/CRC Press.

Frankel, A. (1990). Attenuation of high-frequency shear waves in the crust: measurements from New York State, South Africa, and Southern California, *J. Geophys. Res.* 95: 17441–17457.

Malagnini, L., K. Mayeda, R. Uhrhammer, A. Akinci, and R. B. Herrmann (2007). A regional ground-motion excitation/attenuation model for the San Francisco region, *Bull. Seism. Soc. Amer.* 97: 843–862.

Mayeda, K., L. Malagnini, W. S. Phillips, W. R. Walter, and D. Dreger (2005). 2-D or not 2-D, that is the question: A northern California test, *Geophys. Res. Lett.* 32: L12301.

Mayeda, K., A. Hofstetter, J. L. O'Boyle, and W. R. Walter (2003). Stable and transportable regional magnitudes based on coda-derived moment-rate spectra, *Bull. Seis. Soc. Amer.* 93: 224–239.

Phillips, W. S., H. E. Hartse, and J. T. Rutledge (2005). Amplitude ratio tomography for regional phase Q, *Geophys.Res.Lett.* 32: L21301.

Shih, X. R., K. Y. Chun, and T. Zhu (1994). Attenuation of 1–6 s L_g waves in Eurasia, *J. Geophys. Res.* 99: 23,859–23,875.

Street, R. L., R. B. Herrmann, and O. W. Nuttli (1975). Spectral characteristics of the L_g wave generated by central United States earthquakes, *Geophys. J. R. Astron. Soc.* 41: 51–63.

Taylor, S., A. Velasco, H. Hartse, W. S. Philips, W. R. Walter, and A. Rodgers (2002). Amplitude corrections for regional discrimination, *Pure. App. Geophys.* 159: 623–650.

Venables, W. N. and B. D. Ripley (2002). *Modern Applied Statistics with S*. New York: Springer.

Walter, W. R., K. Mayeda, L. Malagnini, and L. Scognamiglio (2007). Regional body-wave attenuation using a coda source normalization method: Application to MEDNET records of earthquakes in Italy, *Geophys. Res. Lett.* 34: L10308.

Xie, J., R. Gok, J. Ni, and Y. Aoki, (2004). Lateral variations of crustal seismic attenuation along the INDEPTH profiles in Tibet from Lg Q inversion, *J. Geophys. Res.* 109: B10308.

Xie, J. and B. J. Mitchell (1990). Attenuation of multiphase surface waves in the Basin and Range Province. Part I: Lg and Lg coda, *Geophys. J. Int.* 102: 121–137.

Xie, J. (2002). Lg Q in the eastern Tibetan Plateau, *Bull. Seis. Soc. Amer.* 92: 871–876.

Xie, J. (1998). Spectral inversion of Lg from earthquakes: A modified method with applications to the 1995, western Texas earthquake sequence, *Bull. Seis. Soc. Amer.* 88: 1525–1537.

Yoshimoto, K., H. Sato, and M. Ohtake (1993). Frequency-dependent attenuation of P and S waves in the Kanto area, Japan, based on the coda-normalization method, *Geophys. J. Int.* 114: 165–174.